

Millimeter-wave complex conductivity of some epitaxial $\text{YBa}_2\text{Cu}_3\text{O}_{7-\delta}$ films

P. H. Kobrin, W. Ho, W. F. Hall, P. J. Hood, I. S. Gergis, and A. B. Harker

Rockwell International Science Center, Thousand Oaks, California 91360

(Received 16 March 1989; revised manuscript received 23 May 1990)

The first complex conductivities (σ^*) of epitaxial and partly oriented Y-Ba-Cu-O films have been measured at 60 GHz. For the epitaxial films, the real part of the conductivity, σ_1 , shows a maximum just below the superconducting transition. The qualitative behavior of σ^* is not consistent with classical BCS calculations for a homogeneous superconducting film. Large variations in the temperature dependence of σ^* among these films suggest that they are mixtures of normal and superconducting regions. A surface resistance of $10^{-3} \Omega$ at 38 K and a penetration depth of $0.4 \mu\text{m}$ at 55 K have been determined.

INTRODUCTION

Knowledge of the high-frequency response of high- T_c superconductors is important both for technological applications and for a basic understanding of these new materials. Most of the studies to date have been microwave surface resistivity measurements of unoriented bulk ceramics and unoriented films. There have been, however, a few high-frequency measurements of (oriented) single crystals¹ and oriented thin films^{2,3} of $\text{YBa}_2\text{Cu}_3\text{O}_{7-\delta}$ (Y-Ba-Cu-O). In a previous publication,⁴ we described a method to measure the real and imaginary parts of the millimeter-wave complex conductivity ($\sigma^* = \sigma_1 - i\sigma_2$) of superconducting thin films. That study of several oriented multiphase Bi-Ca-Sr-Cu-O films at 62.4 GHz showed a temperature dependence of the complex conductivity which could be explained in terms of superconducting grains nucleating in a normal conducting matrix. This report describes measurement results of the complex conductivity of three highly oriented epitaxial films and one partly oriented film of Y-Ba-Cu-O on single-crystal MgO(100) substrates.

FILM FABRICATION

Epitaxial Y-Ba-Cu-O films 0.065, 0.13, and $0.55 \mu\text{m}$ thick (henceforth referred to as films *A*, *B*, and *C*, respectively) were deposited onto 650°C $1.9 \times 1.9 \times 0.08 \text{ cm}^3$

MgO substrates by ion-beam sputtering from a single ceramic target. After deposition, the films were shiny and x-ray-diffraction (XRD) analysis indicated that they were highly crystalline with the *c* axis oriented perpendicular to the substrate surface. Annealing the epitaxial films for 1 h at 850°C in one atmosphere of oxygen decreased the *c*-axis lattice constant from 11.85 to 11.74–11.79 Å and increased the zero-resistance temperature from $< 30 \text{ K}$ to 56–70 K. The films retained their mirrorlike finish. The *c*-axis lattice constants for each film can be found in Table I. Figure 1(a) shows the Cu $K\alpha$ XRD pattern of film *A*. No *a* axis oriented or unoriented Y-Ba-Cu-O lines are detected. The XRD pattern of film *B* is of equal quality, while film *C* shows a very small line near 33° indicative of residual unoriented Y-Ba-Cu-O.

Film *D* was deposited onto a 20°C MgO substrate from the same target as films *A*–*C* and was then annealed for 20 min at 910°C . After annealing, the film did not have a mirrorlike finish. The XRD pattern of this film is shown in Fig. 1(b). On the same ordinate scale as Fig. 1(a), the 00 l lines are less intense despite the fact that the film is 20 times thicker. The *a* axis and unoriented lines are also more intense. Film *D* can be classified as partly *c* axis oriented.

Ion-coupled plasma atomic emission analysis of epitaxial films from the same target showed the stoichiometry to be within 5% of the correct 1:2:3 ratio. Film *D* has a

TABLE I. Properties of four Y-Ba-Cu-O films.

Film	Thickness (μm)	Growth temp. ($^\circ\text{C}$)	<i>c</i> -Axis Lattice constant (Å)	Sheet resistance			T_c (K) ($R=0$)	ΔT (K) (10–90% ρ_n)	J_c (A/cm ²)
				ρ_n 120 K ($\mu\Omega\cdot\text{cm}$)	dc 120 K (Ω/sq)	60 GHz 120 K (Ω/sq)			
<i>A</i>	0.065	650	11.77	300	45	54	56	11	1×10^6 (35 K)
<i>B</i>	0.13	650	11.74	200	15	14	70	6	1×10^6 (45 K) 5×10^6 (10 K)
<i>C</i>	0.55	650	11.79	290	5.3	4.6	65	11	1×10^6 (40 K) 3×10^6 (10 K)
<i>D</i>	1.3	20	11.69	810	6.3	5.2	70	7	$< 10^3$ (10 K)

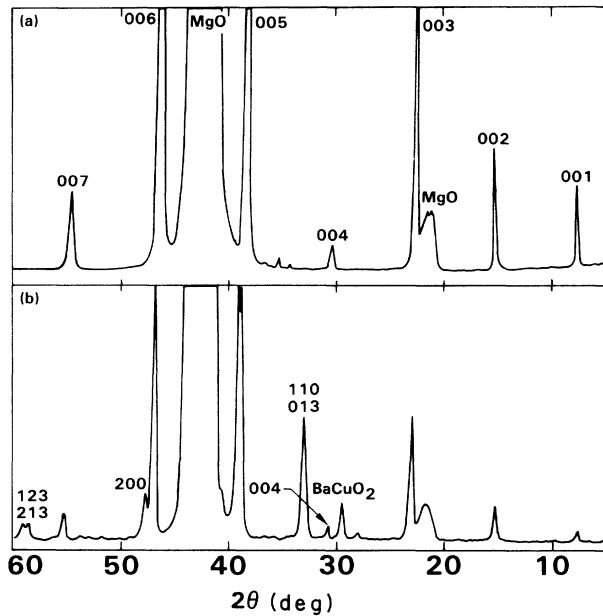


FIG. 1. X-ray-diffraction patterns $\text{Cu } K\alpha$ of (a) film *A*, and (b) film *D*.

Y:Ba:Cu ratio of 1:1.7:2.2. Film thicknesses are based on diamond profilometer measurements ($\pm 20\%$) and, for the thinnest films, are scaled by the duration of deposition. Resistivity measurements were made by the dc four-point probe method. The results are listed in Table I. The resistivity of film *B* is significantly lower than those of films *A* and *C*, while that of film *D* is significantly higher. Film *B* has the sharpest superconducting transition.

By reviewing the literature, it appears that the critical temperature of Y-Ba-Cu-O films grown on MgO substrates are almost universally ~ 10 K lower than films grown on SrTiO_3 . This may be attributed to the MgO thermal expansion coefficient, the lattice constant mismatch and/or to Mg diffusion into the film.⁵ The 56–70 K critical temperature of the films in this work may be further depressed by incomplete oxidation. Later films on MgO from the same target have attained $T_c = 77$ K by annealing to $\sim 900^\circ\text{C}$. Another film from the same target that was grown on LaAlO_3 and annealed to $\sim 900^\circ\text{C}$ had a $T_c = 85$ K.

DC critical currents, J_c , were measured after the millimeter-wave experiments were completed. The films were patterned by ion-milling and gold contacting pads were evaporated and annealed at 650°C to produce low resistance contacts. The results are listed in Table I. All of the epitaxial films exceed 10^6 A/cm² at low temperatures and film *B* reaches 5×10^6 A/cm² at 10 K.

Despite the low critical temperatures, the films grown at high substrate temperatures are epitaxial and single phased as determined by XRD and achieve critical currents at low temperatures that approach the best reported values on SrTiO_3 substrates. Film *D* is not as well oriented and the critical current is significantly lower.

MILLIMETER-WAVE RESULTS

The millimeter-wave measurement system was described previously.⁴ The system uses quasi-optical techniques to produce a near-diffraction-limited beam that is focused onto a sample mounted in a cryogenic stage. The stage has a minimum temperature of 38 K. The intensity and relative phase of the radiation transmitted through the film and substrate are measured. Since the microwave propagation is parallel to the *c* axis of the film the measured properties are those of the *a-b* plane. With a 10 mW millimeter-wave source, the measurable dynamic range in transmission is approximately -60 dB. Relative phases are resolvable to $\pm 1^\circ$ for signal attenuation up to -45 dB, and degrade to $\pm 5^\circ$ at -50 dB. At higher attenuation levels, residual stray millimeter-wave radiation and electronic pickup make the phase measurement unreliable.

Figure 2(a) shows the 60 GHz transmission of the four films. The slopes of the transmission over the normal-state temperature range (300 to 80 K) follow directly the slopes of the four-point dc resistivity measurements made across the entire films. Over this temperature range, the millimeter-wave σ_1 agrees with dc values to better than 20%. The transmission drops dramatically near the superconducting transition. Film *B* shows the largest change, while films *A* and *C* are quite similar. In contrast, the results for film *D* are distinctly different, with a

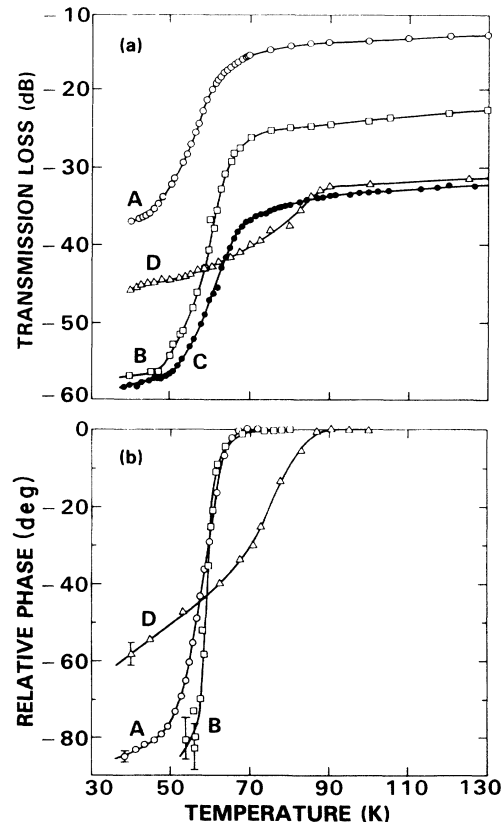


FIG. 2. (a) Transmission loss and (b) relative phase of 58.9 GHz radiation transmitted through films *A–D*.

much smaller transmission change which occurs over a broader temperature interval, similar to those observed for oriented Bi-Ca-Sr-Cu-O (Ref. 4) and other partly oriented Y-Ba-Cu-O films.

Figure 2(b) shows the relative change in phase for the 60 GHz radiation transmitted through films *A*, *B*, and *D*. The phase change for film *C* is very similar to that for film *B* and was omitted for clarity. The large signal attenuation occurring in films *B* and *C* at low temperatures did not allow for phase measurements to be made down to 38 K. Total phase changes of over 80°, approaching the maximum of 90° expected for a fully superconducting thin film with $|\sigma_2| \gg \sigma_1$, were observed for the epitaxial films. The phase change in film *D* is much smaller and occurs over a much broader temperature range.

Analysis of the transmission and phase data was done using an exact multilayer transmission expression, including the known properties of the MgO substrate. The epitaxial films display a common behavior. The relative dielectric constant $\epsilon' = \sigma_2 / \epsilon_0 \omega$ shown in Fig. 3 is negligible above T_c , becomes negative as the film becomes superconducting and approaches large negative values exceeding 10^6 at low temperatures. Concurrently σ_1 (shown in Fig. 4) increases, reaches a maximum and then decreases. For film *A*, where the phase could be measured down to 38 K, σ_1 drops an order of magnitude from its maximum. The complex conductivity of film *D* shows qualitatively different behavior. Although the T_c is as high as that of the best epitaxial film in this study, $\sigma_2 / \epsilon_0 \omega$ drops more slowly and only reaches -2×10^5 . σ_1 shows a very broad maximum and has not dropped appreciably by 38K. Thus, the complex conductivity of film *D* shows greater similarity to those of the Bi-Ca-Sr-Cu-O films in our previous study⁴ than to that of the epitaxial Y-Ba-Cu-O films.

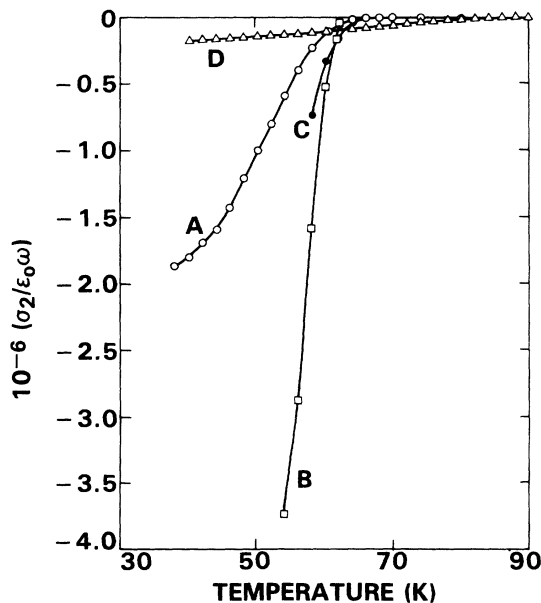


FIG. 3. The computed real dielectric constant ($\sigma_2 / \epsilon_0 \omega$) of films *A*–*D*.

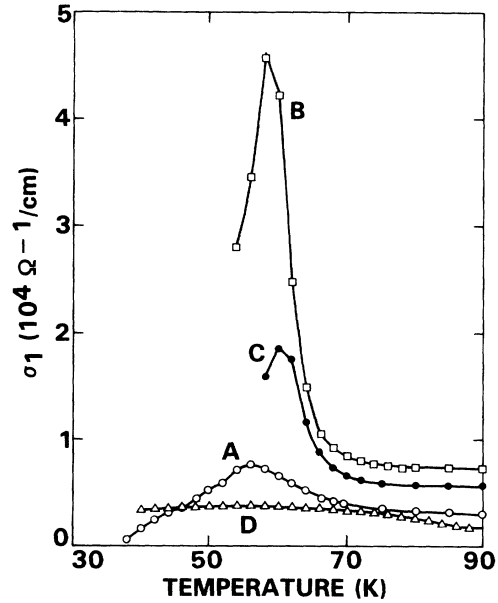


FIG. 4. Computed values of the real conductivity σ_1 for films *A*–*D*.

The penetration depth λ and surface resistance R_s can be calculated from the complex conductivity using

$$1/\lambda = \text{Im}(\omega i \sigma^* / c^2 \epsilon_0)^{1/2}$$

and

$$R_s = \text{Re}(i \omega \mu_0 / \sigma^*)^{1/2} .$$

The calculated surface resistances of the four films are compared in Fig. 5(a) with the surface resistance of

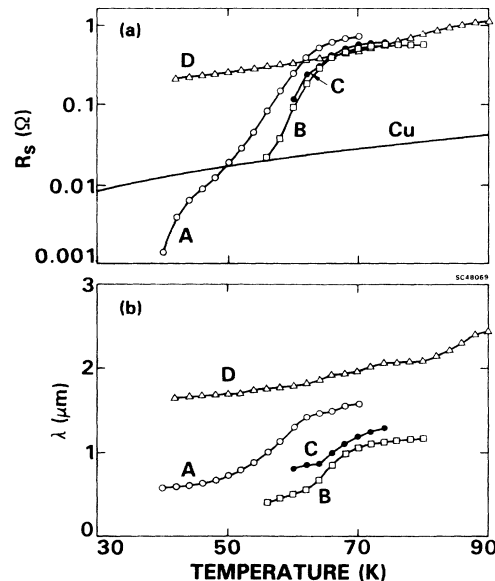


FIG. 5. Calculated values of (a) surface resistance and (b) penetration depth of films *A*–*D*.

copper.⁶ R_s for film *A* drops to 10^{-3} Ω at 38 K which is already an order of magnitude lower than that of copper and is still dropping. These results are comparable to recent surface resistance measurements on Y-Ba-Cu-O films³ (8×10^{-3} Ω at 77 K and 87 GHz) and single crystals¹ (1×10^3 Ω at 77 K and 1.5×10^{-3} Ω at 2 K and 6 GHz) when they are scaled in frequency using an ω^2 BCS model dependence. The R_s of the thicker epitaxial films (*B* and *C*) drop faster than that of film *A*, but the increased attenuation prevented phase measurement at the lower temperatures. With present sensitivity, a film thickness of less than 0.1 μm is required to measure these lower R_s values. The penetration depths for fields in the plane of the film are plotted in Fig. 5(b). The lowest value is 0.4 μm at 55 K for film *B*. This can be compared to low-temperature asymptotic values of 0.14 μm for a bulk ceramic,⁷ and 0.14 μm parallel and 0.7 μm perpendicular to the *ab* plane for a single crystal.⁸ Harshman *et al.*⁸ also report an in-plane penetration depth of 0.26 μm for a ($T_c \sim 65$ K) oxygen-deficient single crystal.

DISCUSSION

The range of microwave and dc electrical properties exhibited by these films demonstrates that significant process variations have occurred, even among the three films (*A*, *B*, and *C*) showing identical degree of orientation.

Since none of the films contain detectable amounts of a second phase, the most reasonable hypothesis is that small differences in oxygen stoichiometry and impurity concentration are responsible for the observed variation. There is a common granular microstructure for these films, and one can expect compositional differences from grain to grain, as well as between the grain interior and its boundary. In addition, in film *D* a significant fraction of the grains are not oriented with *c* axis normal to the film. Since the grains in these films are small compared to the microwave wavelength, the overall electrical response of the film at a finite temperature should be that of a composite medium consisting of superconducting grains in various stages of their transition, intermixed with normal grains.

The microwave response of a superconducting film has been derived from classical BCS theory by Chang and Scalapino⁹ for a 90 K BCS superconductor with electron mean free path *l* as a parameter. This behavior is compared with our experimental data in Figs. 6 and 7 by scaling with the temperature to T_c . The theory depends on microwave frequency through the ratio $h\omega/kT_c$, so we have used their published results at 100 GHz to compare with our data at 60 GHz.

If all the material in the film possessed the same T_c , the microwave response of each film should show the abrupt onset indicated in these figures, with a moderate rise in

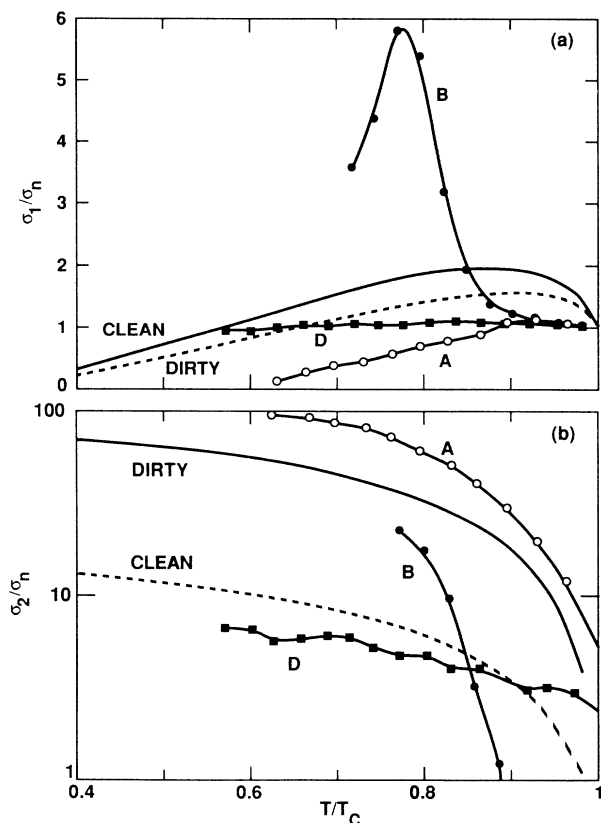


FIG. 6. BCS calculations from Ref. 9 and the measured values of the (a) real and (b) imaginary parts of the complex conductivity normalized to the normal-state conductivity. The temperatures are normalized to the T_c values listed in Table I.

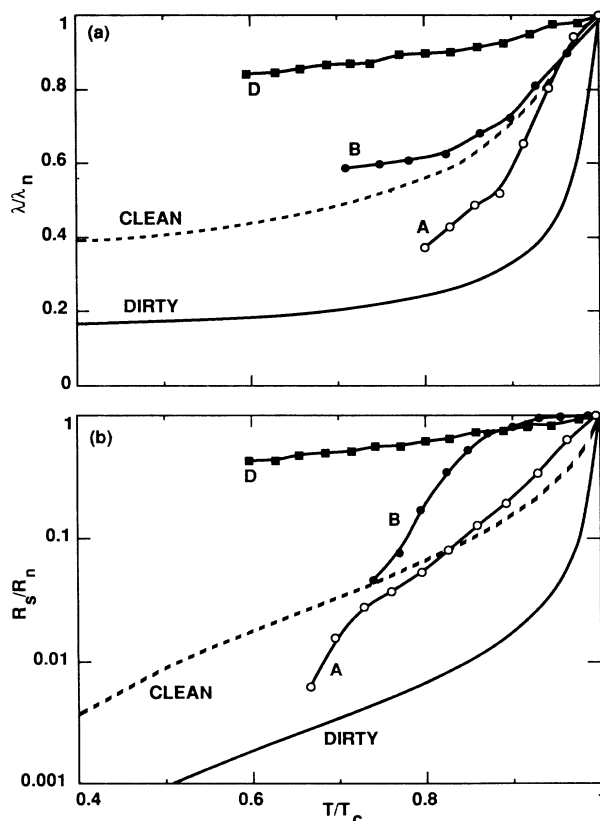


FIG. 7. BCS calculations (Ref. 9) and measured values of the normalized (a) surface resistance, and (b) penetration depth.

σ_1 spread over about 20% of T_c . Instead, for all films both R_s and λ roll off smoothly from their normal-state values, while σ_1 for films *B* and *C* (not shown) rises further and falls faster than this BCS model predicts. This qualitative difference is exactly what one expects from a spread in critical temperatures for the grains. Provided σ_2 rises quickly to large values in the superconducting grains, any composite model^{4,10,11} will predict a corresponding increase in the σ_1 , due to an effective expulsion of the microwave electric field from these grains into the remaining normal material, whose volume fraction is tending to zero. In an earlier paper⁴ we have illustrated this behavior for the extreme case of vanishing σ_1 inside the superconducting grains.

Unfortunately, this folding together of grain σ_1 and σ_2 in the transition region greatly complicates any attempt to infer their intrinsic behavior near T_c . An additional variable, the superconducting volume fraction $\phi(T)$, now enters into the analysis, but there is no additional measurement available to determine it.

At temperatures well below the transition region, all of the grains should be superconducting. However, there is good evidence from cavity resonance measurements that

Y-Ba-Cu-O thin films exhibit much higher surface resistances below $T_c/2$ than is predicted by BCS theory.¹² This has been explained¹³ by hypothesizing that the grains in these films are separated by Josephson junction links, even at 4 K. The microwave response of this complex structure is essentially that of a composite dielectric with an intergranular phase of negative permittivity. Comparable behavior was found in granular NbN films which had been processed to convert the grain boundaries into insulating niobium oxides.¹⁴

In conclusion, the measured microwave and dc electrical properties of Y-Ba-Cu-O films do not yet provide direct tests of superconductivity theories because they appear to be composites whose dielectric behavior is very sensitive to the amount and nature of the nonsuperconducting second phase.

Recently the complex conductivity of $\text{YBa}_2\text{Cu}_3\text{O}_{7-\delta}$ films on MgO substrates produced by other techniques in our laboratory have been measured. These films had T_c 's above 86 K. While the temperature dependence of σ_1 was still qualitatively different from the classical BCS calculations, the penetration depth could be fit quite well by $\lambda = \lambda_0(1 - t^4)^{-1/2}$ with $\lambda_0 = 1750 \text{ \AA}$.

- ¹D. L. Rubin, K. Green, J. Gruschus, J. Kirchgessner, D. Moffat, H. Padamsee, J. Sears, Q. S. Shu, L. F. Schneemeyer, and J. V. Waszczak, *Phys. Rev. B* **38**, 6538 (1988).
- ²J. P. Carini, A. M. Awasthi, W. Beyermann, G. Gruner, T. Hylton, K. Char, M. R. Beasley, and A. Kapitulnik, *Phys. Rev. B* **37**, 9726 (1988).
- ³N. Klein, G. Muller, H. Piel, B. Roas, L. Schultz, U. Klein, and M. Peiniger, *Appl. Phys. Lett.* **54**, 757 (1989).
- ⁴W. Ho, P. J. Hood, W. F. Hall, P. Kobrin, A. B. Harker, and R. E. DeWames, *Phys. Rev. B* **38**, 7029 (1988).
- ⁵T. Komatsu, H. Meguro, R. Sato, O. Tanaka, K. Matsuita, and T. Yamashita, *Jpn. J. Appl. Phys.* **27**, L2063 (1988).
- ⁶R. B. Stewart and V. J. Johnson, Wadd Technical Report No. 60-56, Part IV, 1961 (unpublished).
- ⁷D. R. Harshman, G. Aeppli, E. J. Ansaldo, B. Batlogg, J. H.

- Brewer, J. F. Carolan, R. J. Cava, M. Celio, A. C. D. Chaklader, W. N. Hardy, S. R. Kretzman, G. M. Luke, D. R. Noakes, and M. Senba, *Phys. Rev. B* **36**, 2386 (1987).
- ⁸D. R. Harshman, L. F. Schneemeyer, J. V. Waszczak, G. Aeppli, R. J. Cava, B. Batlogg, L. W. Rupp, E. J. Ansaldo, and D. L. Williams, *Phys. Rev. B* **39**, 851 (1989).
- ⁹J. J. Chang and D. J. Scalapino, *Phys. Rev. B* **40**, 4299 (1989).
- ¹⁰J. Garner and D. Stroud, *Phys. Rev. B* **28**, 2447 (1983).
- ¹¹J. I. Gittleman and J. R. Matey, *J. Appl. Phys.* **65**, 688 (1989).
- ¹²J. Carini, L. Drabeck, and G. Gruner, *Mod. Phys. Lett. B* **3**, 5 (1989).
- ¹³T. L. Hylton, A. Kapitulnik, M. R. Beasley, J. P. Carini, L. Drabeib, and G. Gruner, *Appl. Phys. Lett.* **53**, 1343 (1988).
- ¹⁴D. R. Karecki, G. L. Carr, S. Perkowitz, D. U. Gubser, and S. A. Wolf, *Phys. Rev. B* **27**, 5460 (1983).